Robust Restoration Method for Active Distribution Networks

Xin Chen, Wenchuan Wu, *Senior Member, IEEE*, Boming Zhang, *Fellow, IEEE*

***Abstract*-- Distributed generations (DGs) introduce significant uncertainties to restoration of active distribution networks, in addition to roughly estimated load demands. An adjustable robust restoration optimization model with a two-stage objective is proposed in this paper, involving the uncertain DG outputs and load demands. The first stage generates optimal strategies for recovery of outage power and the second stage seeks the worst-case fluctuation scenarios. The model is formulated as a mixed integer linear programming problem and solved using the column-and-constraint generation method. The feasibility and reliability of the strategies obtained via this robust optimization model can be guaranteed for all cases in the predefined uncertainty sets with good performance. A technique known as the uncertainty budget is used to adjust the conservativeness of this model, providing a tradeoff between conservativeness and robustness. Numerical tests are carried out on the modified PG&E 69-bus system and a modified 246-bus system to compare the robust optimization model against a deterministic restoration model, which verifies the superiority of this proposed model.**

***Index Terms*-- Active distribution network, service restoration, robust optimization.**

NOMENCLATURE

A. Sets

Φ_l	Set of branches.
Ψ_b	Set of buses.
Ψ_{con}	Set of buses in the connected area.
Ψ_{out}	Set of buses in the outage area.
Ψ_{dg}	Set of buses connected with distributed generations.

B. Branch Variables and Parameters

p_{ji}, q_{ji}	Active, reactive power flow from bus *j* to bus *i*.
$\overline{s}_{ij}$	Apparent power capacity of branch *ij*.
z_{ij}	Binary status variable of branch *ij*.
r_{ij}, x_{ij}	Resistance, reactance of branch *ij*.

C. Bus Variables and Parameters

$\tilde{P}_i$, $\tilde{Q}_i$	Actual active, reactive load demand at bus *i*.
P_i^E, Q_i^E	Expected active, reactive load demand at bus *i*.
$(P_i^E - \underline{\hat{P}}_i)$	Lower limit of active load demand at bus *i*.
$(P_i^E + \overline{\hat{P}}_i)$	Upper limit of active load demand at bus *i*.
$\tilde{P}_i^{dg}$	Actual active DG output at bus *i*.
$P_i^{E,dg}$, $Q_i^{E,dg}$	Expected active, reactive DG output at bus *i*.
$(P_i^{E,dg} - \underline{\hat{P}}_i^{dg})$	Lower limit of active DG output at bus *i*.
$(P_i^{E,dg} + \overline{\hat{P}}_i^{dg})$	Upper limit of active DG output at bus *i*.
V_i	Voltage magnitude at bus *i*.
U_i	Squared voltage magnitude at bus *i*.
$\underline{U}_i$, $\overline{U}_i$	Lower, upper limit of squared voltage magnitude at bus *i*.
α_i^+, α_i^-	Fluctuation factors of bus *i*.
n_b	Number of all buses.
n_s	Number of substation buses.
n_{dg}	Number of DG buses.

D. Other Notations and Vectors

N	Uncertainty budget of the robust model.
δ	A small positive number.
M	A large positive number.
$j \in i$	Bus *j* connected to bus *i*.
$\boldsymbol{z}$	Vector of switching decisions.
$\boldsymbol{p}$	Vector of the uncertain DG outputs and the uncertain load demands.
$\boldsymbol{\alpha}$	Vector of fluctuation factors.
$\boldsymbol{x}$	Vector of power flow variables.

I. INTRODUCTION

Service restoration is imperative on the occurrence of a distribution network outage. After detection and isolation of faults, the topology structure of the distribution network needs to be reconfigured to restore power to the blackout area through changing the status of switches. Generally, the problem of determining a restoration scheme for a distribution network supply is a multi-objective, combinatorial, non-linear problem with a number of constraints [1]. There have been considerable studies conducted on distribution network restoration, focusing on the efficiency and optimization of restoration methods. In [2]-[5], heuristic approaches were utilized to search for the required solutions. [6] compares four modern heuristic algorithms for effectiveness, including tabu

This work was supported in part by the China Scholarship Council, in part by the Key Technologies Research and Development Program of China (Grant 2013BAA01B01), the National Science Foundation of China (Grant 51477083). The authors are with the Department of Electrical Engineering, Tsinghua University, Beijing 100084, China (email: wuwench@tsinghua.edu.cn, Correspondig author: Wenchuan Wu).

search, reactive tabu search, parallel simulated annealing and genetic algorithm [7] [8]. Neutral network [9] [10], knowledge-based expert systems [11] [12] and mathematical programming [13]-[15] have been applied to this problem as well.

In recent years, distributed generations (DGs) have increased markedly in distribution networks; these comprise photovoltaic and wind power generators, which are the main contributors to active distribution networks (ADNs), but also present a series of threats to consistent power supply [16]. Further development of fault management technology is required to fully utilize ADNs. However, the rapidly increasing penetration of distributed generation mechanisms introduce further uncertainty risks to ADN restoration, due to their volatility and intermittency. In reality, fulfilling the restoration task is a time-consuming process, while the outputs of DG are not fixed, but fluctuate during this procedure. Although significant researches were devoted to forecasting techniques, DG outputs are not easily predicted accurately. Time-varying load demands in the connected area contribute further uncertainties to service restoration processes. Furthermore, because few real-time measurements exist in distribution networks, it is difficult to obtain a reliable and high-quality estimation of all load demands [17]. In real word, fluctuating DG outputs, time-varying load demands and estimation errors of loads are three major sources of uncertainty factors in ADN restoration. As for the corresponding uncertainty risks, poor restoration performance may result in such uncertain conditions when using a deterministic model, even leading to failures under some restoration strategies since of violation of security constraints. For instance, if the load demands in connected area unexpectedly increase, an originally restoration scheme may cause branches overloading or voltage violations. Such un-robust restoration scheme may induce additional customers' outage. Hence, this range of uncertainties present significant challenges to traditional deterministic algorithms in ADN, and a more robust restoration technique is required to ensure the feasibility and reliability of restoration strategies.

Some studies [17]-[19] have introduced fuzzy approaches and probabilistic tools to modeling uncertainty in DG outputs and load demands for restoration. However, the membership functions of fuzzy numbers are chosen by human experience and probability distributions of random variables need to be given. In our previous work [20], a robust restoration decision-making model based on information gap decision theory is proposed to seek robust strategies, while the description of uncertainty in this method is over-simplified. In [21], the uncertainty of load demand is considered for distribution network reconfiguration incorporated optimal power flow.

As mentioned above, the ADN restoration problem is to solve optimal restoration strategies for maximizing the restored load considering the uncertainties of DG outputs and load demands, while satisfying the operating constraints in distribution networks. In this paper, we formulate this issue as a two-stage adaptive robust optimization model, considering the uncertainties in both DG outputs and load demands. A robust restoration strategy means it can satisfy all the operational constraints during restoration if the uncertain DG outputs and load demands vary within predefined bounded uncertainty sets. The main contributions of this paper are as follows.

1) Based on a deterministic restoration model, we develop a two-stage robust restoration optimization model (RROM), where the fluctuant DG outputs and load demands in ADN are described as predefined uncertainty sets. The bounds of these uncertainty sets can be constructed from profiles of historical data and the operators' needs. In this robust optimization model, the first stage is associated with switching decisions, when we generate the optimal restoration strategy under a certain given scenario. In the second stage, the worst-case fluctuation scenario is sought within the predefined uncertainty sets. The robustness of the restoration strategies generated from this model can be guaranteed for all cases in the uncertainty sets with acceptable optimization performances, which is validated using numerical tests.
2) The original robust restoration optimization model is a mixed integer quadratic constraint programming (MIQCP) model with a two-stage objective function. To facilitate the solving of this model, a quadratic constraint linearization method is adopted to transform the MIQCP to a mixed integer linear programming (MILP) model.

Moreover, the strategy of the uncertainty budget or the price of robustness [22] is introduced to adjust the global range of uncertainty sets, which can control the conservativeness of this model and make a tradeoff between robustness and conservativeness.

Besides this work, there is another robust ADN restoration decision-making model which is based on an information gap decision theory (IGDT-RRDM) [20].The proposed RROM has following two advantages over IGDT-RRDM, which is also the motivation to develop RROM in this paper.

(1) Optimality: The restoration strategies obtained via IGDT-RRDM can ensure feasibility and that the objective does not fall below a certain threshold, whereas they are usually not optimal but just robust feasible solutions, while RROM can always generate robust optimal solutions under the given uncertainty sets in restoration, which is verified by the simulation results.

(2) Applicability: Confronting a fault in ADN, IGDT-RRDM can only provide a specific Pareto optimal front, in which every point is associated with a series of parameters and a certain restoration strategy. However, how to choose optimal values of parameters for IGDT-RRDM is an empirical problem in real application, and there are no general rules to follow. Furthermore, each potential fault in consideration is corresponding to a particular Pareto optimal front with given demand coefficient, so it is rather difficult to gain a complete knowledge base of all these fronts in reality. In contrast, only the uncertainty sets need to be given for RROM according to the profiles of historical data. Therefore, it is much easier for the application of RROM comparing against IGDT-RRDM.

The remainder of this paper is organized as follows. In Section II, a deterministic restoration model and a robust restoration optimization model are presented. In Section III, we use the column-and-constraint generation method to solve this two-stage robust model. Numerical tests are discussed in Section IV, and we draw conclusions in Section V.

II. Robust restoration Model

A. Deterministic Restoration Optimization Model (DROM)

After isolating the faults in a distribution network, supply restoration is conducted to recover the power in unfaulted but out-of-service areas. Essentially, the restoration strategy is an optimal combination of open and closed switches for certain objectives with operating constraints. Based on the studies in [13] and [20], we formulate ADN restoration as a mixed integer quadratic constraint programming model, whose objective is to maximize the restored power. Because the DG outputs and load demands are modeled as constant parameters during the restoration period, it is a deterministic optimization model without regard to uncertainty indeed, which is presented as follows.

1) Objective Function:

$$Obj.\ \ \text{Max} \sum_{i \in \Psi_{out}} \tilde{P}_i \tag{1}$$

$\tilde{P}_i$ is the actual active load demand at bus *i* during the restoration process, and Ψ_{out} is the set of buses in the outage area.

2) Radial Operation Constraint:

$$s.t. \begin{cases} z_{ij} \in \{0,1\},\ \forall (ij) \in \Phi_l \\ \sum_{(ij)\in\Phi_l} z_{ij} = n_b - n_s \end{cases} \tag{2}$$

Binary variable z_{ij} represents the status of branch *ij*, equals to 1 if branch *ij* is connected, and equals to 0 otherwise. Φ_l is the set of all branches. n_b and n_s are the number of all buses and the number of substation buses respectively. Equation (2) ensures no loops in the network [23].

3) Power Balance Constraint at Buses

$$\begin{cases} \sum_{j\in i} p_{ji} = P_i^E, \sum_{j\in i} q_{ji} = Q_i^E \\ \delta \le P_i^E, Q_i^E,\ \forall i \in \Psi_{con} \end{cases} \tag{3}$$

$$\begin{cases} \sum_{j\in i} p_{ji} = \tilde{P}_i, \sum_{j\in i} q_{ji} = \frac{Q_i^E}{P_i^E}\tilde{P}_i \\ \delta \le \tilde{P}_i \le P_i^E, \forall i \in \Psi_{out} \end{cases} \tag{4}$$

$$\begin{cases} \sum_{j\in i} p_{ji} = P_i^{E,dg} / Q_i^{E,dg} \cdot \sum_{j\in i} q_{ji} \\ -P_i^{E,dg} \le \sum_{j\in i} p_{ji} \le -\delta,\ \forall i \in \Psi_{dg} \end{cases} \tag{5}$$

Equations (3)-(5) represent the power balance of buses in connected area, buses in the outage area and DG buses, respectively. p_{ji} and q_{ji} are the active and reactive power flows from bus *j* towards bus *i*, respectively. $\tilde{P}_i$ is the actual active load demand at bus *i* during the restoration period, while P_i^E and Q_i^E are the expected active and reactive load demands at bus *i*, respectively, which are given deterministic parameters. $P_i^{E,dg}$ and $Q_i^{E,dg}$ are the expected active and reactive outputs of the DG, respectively. In equation (4) (5), we presume that the power factors of load demands and DG outputs are fixed during the restoration period. It should be noted that δ denotes a small positive number, and the corresponding inequalities aim to avoid the existence of transfer buses with no generation or load in the solutions.

4) Branch Capacity Constraint

$$p_{ij}^2 + q_{ij}^2 \le z_{ij} \cdot \bar{s}_{ij}^2,\ \ \forall (ij) \in \Phi_l \tag{6}$$

$\bar{s}_{ij}$ is the apparent power capacity of branch *ij* in equation (6), where z_{ij} is added to limit the power flow to zero in disconnected branches.

5) Voltage Security Constraint

$$\begin{cases} U_i = V_i^2 \\ \underline{U}_i \le U_i \le \bar{U}_i,\ \forall i \in \Psi_b \end{cases} \tag{7}$$

In equation (7), V_i is the voltage magnitude at bus *i*. To linearize the quadratic voltage constraint, we use the squared voltage magnitude U_i to represent the voltage variable. $\underline{U}_i$ and $\bar{U}_i$ are the lower and upper limits of the squared voltage magnitude at bus *i*, respectively.

6) Power Flow Equality Constraint

$$\begin{cases} m_{ij} = (1 - z_{ij}) \cdot M \\ U_i - U_j \le m_{ij} + 2(p_{ij} r_{ij} + q_{ij} x_{ij}) \\ U_i - U_j \ge -m_{ij} + 2(p_{ij} r_{ij} + q_{ij} x_{ij}) \\ \forall (ij) \in \Phi_l \end{cases} \tag{8}$$

Equation (8) describes the power flow equations, where power loss in branches is ignored. A big *M* is introduced to cancel the constraints in disconnected branches.

A detailed description of DROM is given in [20].

B. Robust Restoration Optimization Model (RROM)

Based on DROM, we take the uncertainties of the DG outputs and load demands in restoration into account, describing them as predefined polyhedral uncertainty sets $\boldsymbol{\Pi}$:

$$\boldsymbol{\Pi} = \begin{cases} \tilde{P}_i \in \left[P_i^E - \underline{\hat{P}}_i,\ P_i^E + \bar{\hat{P}}_i \right], \forall i \in \Psi_{con} \\ \tilde{P}_i^{dg} \in \left[P_i^{E,dg} - \underline{\hat{P}}_i^{dg},\ P_i^{E,dg} + \bar{\hat{P}}_i^{dg} \right], \forall i \in \Psi_{dg} \end{cases} \tag{9}$$

The restoration problem is then formulated as a two-stage robust optimization model. In the first stage, we generate optimal restoration strategies to maximize the restored power, where switching decisions $\boldsymbol{z}$ are regarded as the decision variables. The worst-case fluctuation scenarios that jeopardize load recovery are sought among the predefined uncertainty sets in the second stage. Following confirmation of the worst-case scenario, we make optimal decisions to restore as much outage load as possible, which gives the final restoration strategy. Accordingly, the formulation of the robust restoration optimization model is presented as follows.

$$Obj.\ \ \max_{\boldsymbol{z}\in\Omega} \left[\min_{\boldsymbol{p}\in\boldsymbol{\Pi}} \left(\text{Max} \sum_{i\in\Psi_{out}} \tilde{P}_i \right) \right] \tag{10}$$

$$s.t.\ \ (2)(4)(6)(7)(8)(9)$$

$$\begin{cases} \sum_{j\in i} p_{ji} = \tilde{P}_i, \sum_{j\in i} q_{ji} = \dfrac{Q_i^E}{P_i^E}\tilde{P}_i \\ \delta \le \tilde{P}_i, \forall i \in \Psi_{con} \end{cases} \tag{11}$$

$$\begin{cases} \sum_{j\in i} p_{ji} = P_i^{E,dg} \big/ Q_i^{E,dg} \cdot \sum_{j\in i} q_{ji} \\ -\tilde{P}_i^{dg} \le \sum_{j\in i} p_{ji} \le -\delta, \forall i \in \Psi_{dg} \end{cases} \tag{12}$$

The objective function of RROM takes the form of maximizing a minimax problem, where Ω denotes the feasible region of the switching decisions vector $\boldsymbol{z}$, which is a convex set and provides a simple description of radial constraints. The vector $\boldsymbol{p}$ represents the uncertain variables subject to the uncertainty sets $\boldsymbol{\Pi}$, involving the uncertain DG outputs and uncertain load demands. In equation (11), constant power factors of fluctuant load demands are assumed at the connected buses. Since we make decisions under the worst-case scenarios, the restoration strategies obtained via RROM are immune to the uncertainty factors and retain robustness for all cases in the given uncertainty sets.

RROM is a mixed integer quadratic constraint programming (MIQCP) model with a two-stage objective function. To facilitate dualization in the subsequent solving process, the nonlinear model must be linearized; all equations are linear except equation (6), which presents a circular constraint. With the quadratic constraint linearization method shown in Fig. 1, we can use several square constraints to approximate the circular constraint. In this paper, two square constraints (13) are employed to substitute for equation (6), providing an adequate level of precision for engineering applications. In general, the use of more square constraints will increase the accuracy of the approximation. As a consequence of this transformation, RROM becomes a mixed integer linear programming (MILP) model.

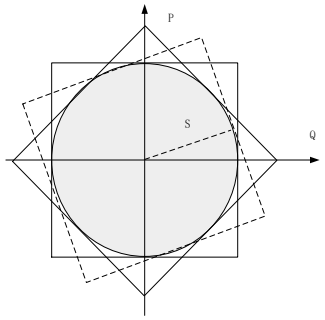

Figure 1. Circular constraint linearization method.

$$\begin{cases} -z_{ij}\cdot\overline{s}_{ij} \le p_{ij} \le z_{ij}\cdot\overline{s}_{ij} \\ -z_{ij}\cdot\overline{s}_{ij} \le q_{ij} \le z_{ij}\cdot\overline{s}_{ij} \\ -\sqrt{2}z_{ij}\cdot\overline{s}_{ij} \le p_{ij}+q_{ij} \le \sqrt{2}z_{ij}\cdot\overline{s}_{ij} \\ -\sqrt{2}z_{ij}\cdot\overline{s}_{ij} \le p_{ij}-q_{ij} \le \sqrt{2}z_{ij}\cdot\overline{s}_{ij} \\ \forall (ij) \in \Phi_l \end{cases} \tag{13}$$

Nevertheless, searching for the worst-case fluctuation scenarios across the whole of the uncertainty sets may result in rather conservative strategies and risk losing optimality. To address this issue, the uncertainty budget [22] approach is utilized to control the conservativeness of RROM. The uncertainty sets are parameterized as expression (14) with auxiliary variables $\{\alpha_i^+, \alpha_i^-\}$ called fluctuation factors. Another constraint equation (15) is added to serve as the uncertainty budget.

$$\boldsymbol{\Pi}' = \begin{cases} \tilde{P}_i = P_i^E + \alpha_i^+ \overline{\hat{P}}_i - \alpha_i^- \underline{\hat{P}}_i \\ \tilde{P}_i^{dg} = P_i^{E,dg} + \alpha_i^+ \overline{\hat{P}}_i^{dg} - \alpha_i^- \underline{\hat{P}}_i^{dg} \\ \alpha_i^+ \in [0,1], \alpha_i^- \in [0,1] \\ \forall i \in \{\Psi_{con}, \Psi_{dg}\} \end{cases} \tag{14}$$

$$\sum_{i\in\{\Psi_{con},\Psi_{dg}\}} \left(\alpha_i^+ + \alpha_i^-\right) \le N \tag{15}$$

In equation (14), fluctuation factors $\{\alpha_i^+, \alpha_i^-\}$ are normalized variables, describing the upward or downward degree of deviations from the expected values. In equation (15), the parameter *N* denotes the uncertainty budget of RROM, and we derive a normalized value *S* called *Robust Strength* for a better description, given by equation (16).

$$S = N \big/ \left(n_{con} + n_{dg}\right) \tag{16}$$

After isolation of faults, the number of fluctuation buses $\left(n_{con} + n_{dg}\right)$ is known in restoration. We can alter the value of the robust strength *S* from zero to one to change the range of the uncertainty sets, and make an adjustment to the global conservativeness of RROM. In particular, when *S* equals zero, RROM is identical to DROM, and the worst-case scenarios in the overall given uncertainty sets are considered if *S* equals one.

III. Solution of The Robust Restoration Optimization Model

To make the solution algorithm explicit, we express the formulation of RROM in a compact form as follows.

$$Obj.\ \max_{\boldsymbol{z}\in\Omega}\left[\min_{\boldsymbol{p}\in\boldsymbol{\Pi}'}\left(\max \boldsymbol{c}^{\mathrm{T}}\boldsymbol{x}\right)\right] \tag{17}$$

$$s.t.\quad \boldsymbol{A}\boldsymbol{x} \le \boldsymbol{p} \tag{18}$$

$$\boldsymbol{C}\boldsymbol{x} + \boldsymbol{D}\boldsymbol{z} \le \boldsymbol{f} \tag{19}$$

$$\boldsymbol{i}^{\mathrm{T}}\boldsymbol{\alpha} \le N \tag{20}$$

The power flow variables $\{p_{ij}, q_{ij}, U_i\}$ are chosen as the decision vector $\boldsymbol{x}$ in the inner objective, and expression (17) is the same as equation (10). Expression (18) represents the power balance constraints at the DG buses and the connected buses. It should be noted that the equations for power balance are reformulated in an equivalent unified form as inequalities, for simplicity. The remaining equations of the operational constraints are demonstrated in expression (19), and expression (20) describes the uncertainty budget, where the vector $\boldsymbol{\alpha}$ denotes the fluctuation factors in correlation with the uncertainty sets. From expression (14), it is observed that a particular value of $\boldsymbol{\alpha}$ represents a given fluctuation scenario.

Since RROM is a two-stage robust optimization model, we choose to solve this problem using the column-and-constraint

generation method introduced in [24]. According to the different objectives of these two stages, RROM is divided into the master problem and the subproblem, then a master-sub iterative process is followed.

A. Master Problem (MP)

The master problem refers to the first-stage decision in RROM, shown as follows:

$$Obj.\ P_M = \underset{\boldsymbol{z}\in\Omega}{\text{Max}}\ \eta \tag{21}$$

$$s.t.\ \begin{cases} \eta \le \boldsymbol{c}^{\mathrm{T}}\boldsymbol{x}^{l} \\ \boldsymbol{A}\boldsymbol{x}^{l} \le \boldsymbol{p}_{*}^{\,l} \\ \boldsymbol{C}\boldsymbol{x}^{l} + \boldsymbol{D}\boldsymbol{z} \le \boldsymbol{f} \\ \forall\, l=1,\ldots,\mathrm{k} \end{cases} \tag{22}$$

In the master problem, the vector $\boldsymbol{p}$ is replaced by the known vector $\boldsymbol{p}_*$ in expression (22), such that the fluctuation scenarios are given as known conditions. This aims to generate optimal restoration strategies for maximization of the restored power under the operational constraints. The uncertainty sets are substituted by finite partial enumeration scenarios with the superscript l, and the optimal value P_M provides an upper bound for the original objective in expression (17). In this manner, the formulation of the master problem is a mixed integer linear programming model, which is a convenient mathematical form for solution.

B. SubProblem (SP)

The subproblem corresponds to the minimax problem in expression (17), which is presented as follows:

$$Obj.\quad P_S = \underset{\boldsymbol{p}\in\boldsymbol{\Pi}'}{\text{Min}}\left(\ \text{Max}\ \boldsymbol{c}^{\mathrm{T}}\boldsymbol{x}\right) \tag{23}$$

$$s.t.\ \begin{cases} \boldsymbol{A}\boldsymbol{x} \le \boldsymbol{p} \\ \boldsymbol{C}\boldsymbol{x} + \boldsymbol{D}\boldsymbol{z}_{*} \le \boldsymbol{f} \\ \boldsymbol{i}^{\mathrm{T}}\boldsymbol{\alpha} \le N \end{cases} \tag{24}$$

In the subproblem, the switching decisions $\boldsymbol{z}_*$ are given as the known conditions in expression (24). The worst-case fluctuation scenario that minimizes the recovered power under given restoration strategies is found, and the optimal value P_S serves as a lower bound for the original objective in expression (17). While the subproblem is a minimax problem, it should be reformulated in a monolithic form through strong duality, shown as follows:

$$Obj.\ P_S = \text{Min}\left[\boldsymbol{\lambda}_1^{\mathrm{T}}\boldsymbol{p} + \boldsymbol{\lambda}_2^{\mathrm{T}}\left(\boldsymbol{f} - \boldsymbol{D}\boldsymbol{z}_{*}\right)\right] \tag{25}$$

$$s.t.\ \begin{cases} \boldsymbol{\lambda}_1^{\mathrm{T}}\boldsymbol{A} + \boldsymbol{\lambda}_2^{\mathrm{T}}\boldsymbol{C} = \boldsymbol{c}^{\mathrm{T}} \\ \boldsymbol{\lambda}_1, \boldsymbol{\lambda}_2 \ge 0 \\ \boldsymbol{i}^{\mathrm{T}}\boldsymbol{\alpha} \le N \end{cases} \tag{26}$$

However, there exist bilinear terms in expression (25). To solve this problem, we force the uncertainty budget N to be an integer. After that, the worst-case fluctuation scenarios must exist at the extreme points of the uncertainty sets, which means that the fluctuation factors α_i^+ and α_i^- must be either one or zero; the proof of this proposition is provided in [25]. Then, a standard linearization technique is applied to handle this problem. We substitute each product $\boldsymbol{\alpha}_i\boldsymbol{\lambda}_i$ with a new variable ω_i, and the big M method is utilized once again for relaxation. Finally, the dual-sub problem is presented as follows.

$$Obj.\ P_S = \text{Min}\left[\left(\boldsymbol{\lambda}_1^{\mathrm{T}}\boldsymbol{p}_E + \boldsymbol{\omega}^{\mathrm{T}}\widehat{\boldsymbol{p}}\right) + \boldsymbol{\lambda}_2^{\mathrm{T}}\left(\boldsymbol{f} - \boldsymbol{D}\boldsymbol{z}_{*}\right)\right] \tag{27}$$

$$s.t.\ \begin{cases} (26) \\ \omega_i \le \boldsymbol{\lambda}_i,\ \omega_i \le M\boldsymbol{\alpha}_i \\ \omega_i \ge \boldsymbol{\lambda}_i - M\left(1 - \boldsymbol{\alpha}_i\right) \\ \omega_i \ge 0,\ \boldsymbol{\alpha}_i \in \{0,1\},\ \forall i \end{cases} \tag{28}$$

In expression (27), the vector $\boldsymbol{p}_E$ denotes the expected DG outputs and load demands, and the vector $\widehat{\boldsymbol{p}}$ represents the predefined deviations of the actual values away from the expected in the given uncertainty sets.

C. C&CG Algorithm

The column-and-constraint generation (C&CG) algorithm procedure [24] for solving RROM is described as follows:

1. *Initialization:*
   · Set LB=0, UB=+∞, k=0;
   · Set the convergence tolerance $\varepsilon \ge 0$.
   · Solve DROM to obtain the initial switching decisions $\boldsymbol{z}^k$ and the optimal objective P_0.
   · Update the upper bound $\text{UB} = \min\{\text{UB}, P_0\}$;
2. *Solving the sub problem (SP):*
   · Given the switching decisions $\boldsymbol{z}^k$, solve SP to obtain the worst-case fluctuation scenario $\boldsymbol{p}_*^{\,k+1}$ and P_S.
   · If $|P_S| < +\infty$, create variables $\boldsymbol{x}^{k+1}$ and add the following constraints to MP.

$$\begin{cases} \eta \le \boldsymbol{c}^{\mathrm{T}}\boldsymbol{x}^{k+1} \\ \boldsymbol{A}\boldsymbol{x}^{k+1} \le \boldsymbol{p}_{*}^{\,k+1} \\ \boldsymbol{C}\boldsymbol{x}^{k+1} + \boldsymbol{D}\boldsymbol{z} \le \boldsymbol{f} \end{cases} \tag{29}$$

   Update the lower bound $\text{LB} = \max\{\text{LB}, P_S\}$.
   · If $|P_S| = +\infty$, create variables $\boldsymbol{x}^{k+1}$ and add the following constraints to MP.

$$\begin{cases} \boldsymbol{A}\boldsymbol{x}^{k+1} \le \boldsymbol{p}_{*}^{\,k+1} \\ \boldsymbol{C}\boldsymbol{x}^{k+1} + \boldsymbol{D}\boldsymbol{z} \le \boldsymbol{f} \end{cases} \tag{30}$$

3. *Solving the master problem (MP):*
   · Solve MP to obtain the switching decisions $\boldsymbol{z}^{k+1}$ and the optimal value P_M.
   · Update the upper bound $\text{UB} = \min\{\text{UB}, P_M\}$.
4. *Checking for convergence* :
   · If $\text{UB} - \text{LB} \le \varepsilon$, terminate.
   · Else $k = k + 1$, and go back to step 2.

The master problem and the dual-sub problem are both mixed integer linear programming models, which can be solved efficiently using many commercially available optimizers, such as IBM CPLEX.

IV. Numerical Tests

In section IV, the characteristics of RROM are demonstrated using numerical tests. At first, we give a brief introduction to the modified PG&E 69-bus test system. Secondly, a performance comparison between DROM and RROM is made in the worst-case fluctuation scenarios and using Monte Carlo simulations. Then, the advantages of RROM over our previous robust model IGDT-RRDM are illustrated through simulation results. Next, we discuss the impact of the uncertainty budget in RROM. Lastly, simulation results of additional testcases carried out on a 246-bus distribution system are provided.

All the programming and numerical tests are implemented in the distribution management system (DMS) developed by Tsinghua University, and the power flow tools based on DMS are used as our simulator, whose core algorithms are revised backward/forward sweep and implicit Z-bus method.

A. Introduction to the PG&E 69-bus Test System

The robust restoration optimization model is tested on a modified PG&E 69-bus system. As shown in Fig. 2, the dashed red lines denote the link lines that are usually open, and the yellow diamonds represent the buses connected to distributed generators. Assuming all branches can be operated, basic information on branch impedances and expected load demands is provided in [26].

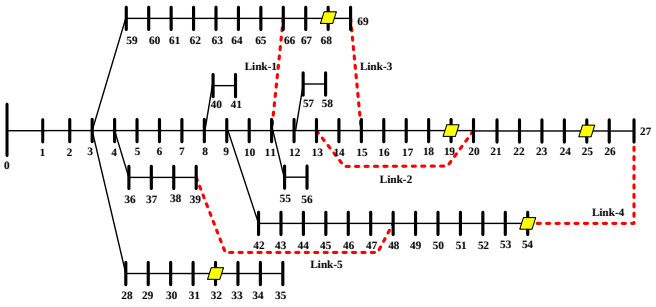

Figure 2. The modified PG&E 69-bus system.

In the test system, we set the voltage of the substation bus to 10.5 kV, and the lower and upper bounds of voltage to 9 kV and 11 kV for all buses, respectively. The apparent power limits of branches are listed in Table I, and Table II presents output information for the DGs.

TABLE I.
Apparent Power Limitation of Branches

Corresponding branches	Apparent power limitation (MVA)
ln26-27,ln34-35,ln68-69,ln38-39, ln40-41,ln53-54,ln55-56,ln57-58	1.12
ln25-26, ln33-34, ln67-68, ln37-38, ln8-40,ln52-53, ln11-55, ln12-57	2.24
ln11-66, ln13-14, ln15-69, ln27-54, ln39-48	3.54
ln21-22,ln22-23,ln23-24, ln30-31,ln31-32, ln32-33, ln36-37,ln6465,ln65-66, ln66-67, ln49-50,ln50-51,ln51-52	4
All other branches	6.5

TABLE II.
Output Information For Distributed Generators

Bus No.	DG Output (kW,kVar)	Bus No.	DG Output (kW,kVar)	Bus No.	DG Output (kW,kVar)
Bus-19	150+j70	Bus-32	40+j25	Bus-68	100+j50
Bus-25	70+j40	Bus-54	6.5+j40	/	/

B. Tests in the Worst-Case Fluctuation Scenarios

In this part, we assumed that the predefined uncertainty sets of DG outputs and load demands were given as expression (31), and the robust strength S in RROM was set to one, which implied that it sought the worst cases in the overall uncertainty sets. We extracted the worst-case fluctuation scenarios from the second stage of RROM, and compared DROM and RROM restoration performances under these conditions.

$$\begin{cases} \tilde{P}_i \in \left[0.65\,P_i^E,\ 1.35\,P_i^E\right], \forall i \in \Psi_{con} \\ \tilde{P}_i^{dg} \in \left[0.7P_i^{E,dg}, 1.3P_i^{E,dg}\right], \forall i \in \Psi_{dg} \end{cases} \tag{31}$$

In the case of a fault occurring in branch 13-14, for example, an outage of 0.368 MW will occur after isolating the fault, and service restoration is conducted using DROM and RROM respectively. If the actual DG output $\tilde{P}_i^{dg}$ and load demand $\tilde{P}_i$ remain constant with the expected $P_i^{E,dg}$ and P_i^E during the restoration period, an unfluctuating scenario is observed. In this case, the DROM and RROM restoration strategies were both successful.

However, under the worst-case fluctuation scenario derived from the second stage of RROM, the DROM strategy failed to recover the outage, since it ignored the uncertainty and caused that the voltage magnitudes of bus-50, bus-51, bus-52, bus-53 and bus-54 were less than 0.9p.u (violating their lower bounds). To implement the DROM restoration scheme, additional 0.0282 MW of load shedding is deemed to occur. In contrast, the strategy generated using RROM recovered the outage in this worst case and achieved an optimal restored power of 0.368 MW. As presented in [26], the excepted load demand at bus-50 is rather heavy, which reaches up to 1244kW+888kvar, so it increases significantly in worst-case scenario. Sharp voltage drop happened among bus-50 and it's downstream when DROM strategy is conducted. Whereas under RROM strategy, branch 49-50 is disconnected and the heavy load is transferred to another major branch, which avoids the voltage violation. This is the specific reason why there are such distinct outcomes between DROM and RROM.

Table III presents the above worst-case fluctuation scenario, and detailed test results are shown in Table IV.

TABLE III.
THE WORST-CASE SCENARIO DERIVED FROM RROM IN THE FAULT OF BRANCH 13-14.

The uncertain load demands: $\tilde{P}_i = \theta_i P_i^E, \forall i \in \Psi_{con}$	
bus-1	$\theta_i = 1$ (forced)
bus-2 and bus-61	$\theta_i = 0.65$
All other buses in the connected area	$\theta_i = 1.35$
The uncertain DG outputs: $\tilde{P}_i^{dg} = \theta_i^{dg} P_i^{E,dg}, \forall i \in \Psi_{dg}$	
All the DG buses	$\theta_i^{dg} = 0.7$

TABLE IV.
RESTORATION RESULTS FOR DROM AND RROM IN BRANCH 13-14 UNDER THE UNFLUCTUATING AND WORST-CASE FLUCTUATION SCENARIOS.

Model	Restoration strategies	Restored power (MW)	
		Unfluctuating scenario	Worst-case scenario
DROM	Disconnected: ln64-65, ln27-54, ln39-48. Other branches are connected.	0.368 (Success)	-0.0282 (Fail: buses 50~54 violate their lower voltage limits)
RROM	Disconnected: ln9-10, ln38-39, ln49-50. Other branches are connected.	0.368 (Success)	0.368 (Success)

Similarly, we undertake an "N-1" restoration scan process in the test system under the worst-case scenarios. In each scan, one branch is assumed to be tripped, and fault isolation and restoration then follow. A performance comparison between DROM and RROM is shown in Fig 3. The dotted green line denotes the restorable power after the isolation of faults, and the solid blue curve and the dashed red curve represent the final restored power of RROM and DROM, respectively. It is clear that RROM is significantly more robust than DROM in the worst-case scenarios. Failures occurred in 27 cases using the DROM strategies, leading to additional load shedding, while the RROM strategies remained feasible and optimal at all times.

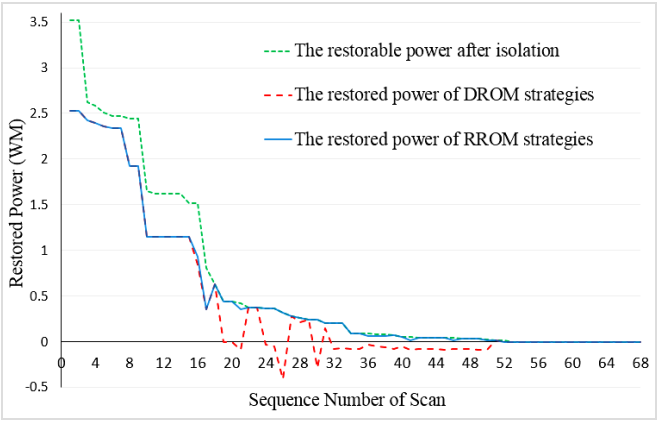

Figure 3. A restoration performance comparison between DROM and RROM under the worst-case fluctuation scenarios. The x-axis is the sequence number of the scan in decreasing order of the restorable power. The y-axis is the final restored power, in units of MW.

Excluding 17 branches with zero restorable power, the restoration results of DROM and RROM are summarized in Table V, where the success rate is the proportion of the cases which were successful among the remaining 51 cases in the "N-1" scan.

TABLE V.
RESTORATION COMPARISON OF DROM AND RROM IN THE "N-1" SCAN UNDER THE WORST-CASE FLUCTUATION SCENARIOS

Model	Number of failures	Success rate	Total restored power (MW)	Number of cases with higher restored power
DROM	27	47.06%	27.69	0
RROM	0	100%	35.09	30

C. Tests Using Monte Carlo Simulations

Monte Carlo simulations were carried out to compare the restoration performances of DROM and RROM under normal conditions. We presume that the actual DG outputs and load demands are independent random variables with Gaussian distributions. Up to 2000 fluctuation scenarios were generated independently and randomly for restoration of each faulty branch, and $\mu \pm 3\sigma$ (μ is the expectation value and σ represents the standard deviation) intervals are ensured in sampling. The robust strength S and the given uncertainty sets of the DG outputs and load demands were identical to those used in Part B.

Another restoration "N-1" scan was conducted in the modified PG&E 69-bus test system using Monte Carto simulations. From the results of this scan, it was observed that the success rate of the RROM strategies was consistently 100%, with a greater average restored power than for the DROM strategies. RROM is clearly more successful for most restoration cases compared to DROM. The simulation results are summarized for five cases in Table VI.

TABLE VI.
MONTE CARLO SIMULATION RESULTS USING DROM AND RROM FOR RESTORATION IN FIVE TYPICAL CASES

Type	Faulty Branch	Model	Success rate	Average restored power $\bar{P}$ (MW)	$\bar{P}_R - \bar{P}_D$ (MW)
I	ln15-16	DROM	71.05%	0.189322	0.133078
		RROM	100%	0.32240	
	ln51-52	DROM	86.05%	0.196572	0.048428
		RROM	100%	0.24500	
II	ln37-38	DROM	100%	0.386334	0.038444
		RROM	100%	0.424778	
III	ln12-13	DROM	100%	0.376	0
		RROM	100%	0.376	
	ln20-21	DROM	100%	0.08740	0
		RROM	100%	0.08740	

With respect to cases of Type I, DROM fails repeatedly and leads to additional load shedding under certain fluctuation scenarios considered using the Monte Carlo simulations. For cases of Type II the DROM strategies remain feasible but their

performance is poor. It is observed that RROM performs better in the above two cases in terms of robustness. Type III denotes the cases in which DROM and RROM have identical restoration performance, with the same average recovered power; these represent most cases in the simulation tests.

D. The Advantages of RROM over IGDT-RRDM

In this part, we make a comparison between RROM and IGDT-RRDM in restoration performance under the worst-case fluctuation scenarios, and explain the advantages of RROM mentioned above through these simulation results. The predefined uncertainty sets of DG outputs and load demands in RROM are similar to Part B. With respect to the parameters of IGDT-RRDM, we set the demand coefficient δ to 0.8 and the fluctuation of DG outputs β to 0.3, with the objective to maximize the fluctuation of load demands α .

Excluding 17 branches with zero restorable power, we conduct an "N-1" restoration scan process in the worst-case fluctuation scenarios again. Fig 4 presents the comparison results between IGDT-RRDM and RROM in restoration performance. The dotted green line denotes the demanded restorable power of IGDT-RRDM, which is a discounted (80%) result of the original optimal objective of DROM. And the solid blue curve and the dashed red curve represent the final restored power of RROM and IGDT-RRDM, respectively.

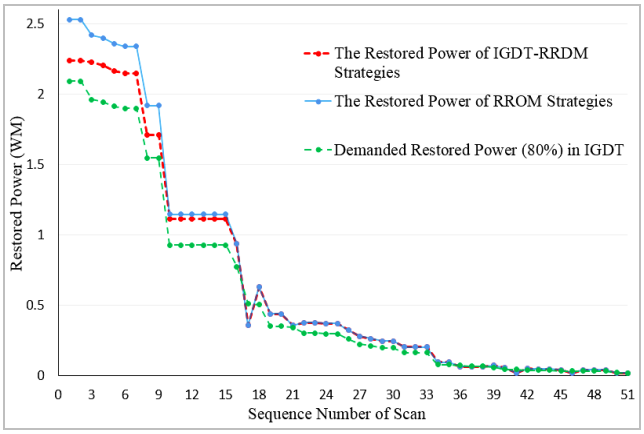

Figure 4. A restoration performance comparison between IGDT-RRDM and RROM under the worst-case fluctuation scenarios. The x-axis is the sequence number of the scan in decreasing order of the demanded restorable power. The y-axis is the final restored power, in units of MW.

It shows that both RROM and IGDT-RRDM strategies kept feasible in all the worst-case scenarios, while RROM performed not worse than IGDT-RRDM in all cases, and achieved higher restored power in 15 cases among them. These results reflect that the strategies generated from IGDT-RRDM may just robust feasible solutions, but not the robust optimal solutions obtained via RROM.

Since IGDT-RRDM can provide a Pareto optimal front with a given δ and each point $[\alpha,\beta,\delta]$ in such front is associated with a particular restoration strategy. Here, we intend to compare RROM against IGDT-RRDM with different values of parameters $[\alpha,\beta,\delta]$ under the worst-case scenarios. Simulation results of three cases are presented as Table VII. The values of parameters in IGDT-RRDM, for example, [0.862, 0.3, 0.8] is corresponding to $[\alpha,\beta,\delta]$ in sequence, and means that α=0.862 , β=0.3 and δ=0.8 . Table VII lists the disconnected branches in restoration strategies, and the other remaining branches are all connected.

From Table VII, it is seen that the strategies obtained via IGDT-RRDM change with different values of $[\alpha,\beta,\delta]$, leading to distinct restored power in simulations. However, only with the best values of parameters, the restoration performance of IGDT-RRDM can match up to RROM's, otherwise an un-optimal strategy will be obtained. In addition, it seems that there is no general rule to use to choose the optimal values for the parameters from the simulation results.

TABLE VII.
RESTORATION RESULTS OF RROM AND IGDT-RRDM WITH DIFFERENT PARAMETERS IN THREE CASES UNDER THE WORST-CASE SCENARIOS.

Faulty Branch	Model		Restored power (MW)	Disconnected branches in restoration strategies
ln7-8	RROM		2.35973	ln11-12, ln13-14, ln49-50, ln39-48.
	IGDT-RRDM	[0.862,0.3,0.8]	2.1665	ln13-20, ln15-69, ln27-54, ln39-48.
		[0.758,0.6,0.8]	2.29259	ln15-16, ln68-69, ln50-51, ln39-48.
		[0.648,0.3,0.9]	2.33045	ln12-13 ln14-15, ln50-51, ln39-48.
		[0.544,0.6,0.9]	2.35973	ln11-12, ln18-19, ln49-50, ln39-48.
ln8-40	RROM		2.3397	ln11-12, ln13-14, ln49-50, ln39-48.
	IGDT-RRDM	[0.758,0.3,0.8]	2.14648	ln13-20, ln15-69, ln27-54, ln39-48.
		[0.661,0.6,0.8]	2.3397	ln11-12, ln19-20, ln49-50, ln39-48.
		[0.559,0.3,0.9]	2.27258	ln16-17, ln50-51, ln15-69, ln39-48.
		[0.462,0.6,0.9]	2.33421	ln12-13, ln15-16, ln49-50, ln39-48.
ln42to43	RROM		1.14528	ln10-11, ln14-15, ln15-16, ln49-50..
	IGDT-RRDM	[0.511,0.3,0.8]	0.935196	ln4-5, ln12-13, ln14-15, ln53-54..
		[0.454,0.6,0.8]	1.11316	ln4-5, ln13-14, ln15-16, ln51-52.
		[0.454,0.3,0.9]	1.11316	ln4-5, ln14-15, ln51-52, ln15-69.
		[0.396,0.6,0.9]	1.11316	ln4-5, ln13-14, ln51-52, ln15-69.

According to the simulation results, robust feasible but not optimal strategies may be generated from IGDT-RRM, while RROM can guarantee the robustness and optimality of its strategies simultaneously, and has apparent superiors over IGDT-RROM.

E. The Impact of the Uncertainty Budget

Using the uncertainty budget given in equation (15), we can tune the value of budget *N* to adjust the conservativeness of RROM. Under the worst-case fluctuation scenarios in the overall uncertainty sets, RROM is utilized for restoration with varying budget *N*. The results of four cases are shown in Fig.4, involving branch 14-15, branch 15-16, branch 18-19 and branch 59-60.

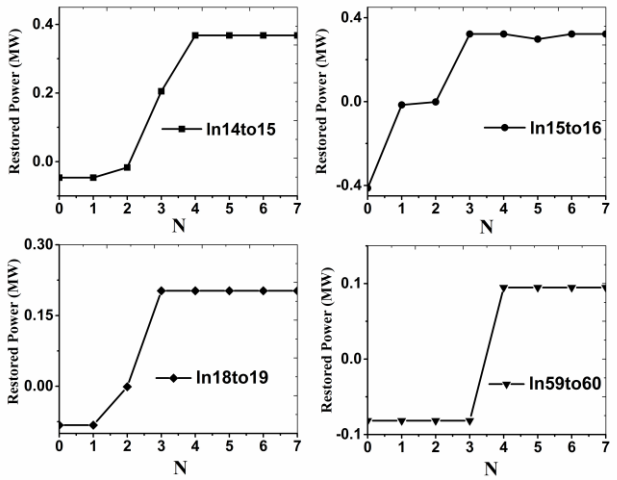

Figure 5. Restoration performance of RROM with varying budget *N* under the worst-case fluctuation scenarios in the whole uncertainty sets. The x-axis is the value of the uncertainty budget *N*, which is a discrete integer. The y-axis is the restored power using RROM strategies with the corresponding budget, whose unit is MW.

From Fig. 5, it is observed that the restored power of RROM increases under the same worst-case scenarios when the budget *N* is increased, consistent with the intuitive result that a larger budget should yield a more robust strategy. In addition, the restored power convergences rapidly with increasing budget, and reaches an optimal value when the budget is set to three or four.

F. Numerical Tests on 246-bus Distribution System

To further illustrate the scalability of the proposed method, RROM has been tested on a larger scale distribution system additionally, which comprises two feeders, 246 buses, 244 branches and 5 link lines in total. As shown in Fig 6, the test system combines two parallel feeders, and each of them follows an identical modified IEEE 123-bus system, presented in Fig 7. The square and the gray rectangles denote the substation bus (marked as "bus-1") and the distribution generations, respectively. These dashed red lines represent the link lines that are usually open, while link line-3 is the one that connects these two feeders from bus-72(A) to bus-72(B). Detailed parameters and configurations of the modified IEEE 123-bus test system are available online [27].

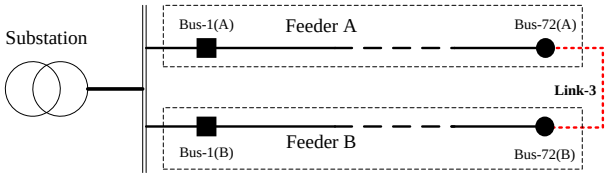

Figure 6. The double-feeder distribution system used for simulation tests (a combination of two IEEE 123-bus systems, shown in Fig 7).

Similarly, we compare RROM against DROM in restoration performance under the worst-case fluctuation and using Monte Carlo simulations. The predefined uncertainty sets of DG outputs and load demands are exactly the same as equation (31), and we assume that all branches can be operated in the restoration procedure. Since the configurations of this double-feeder test system are symmetrical, only the cases when faults occurs on Feeder A are under consideration in the following simulation tests.

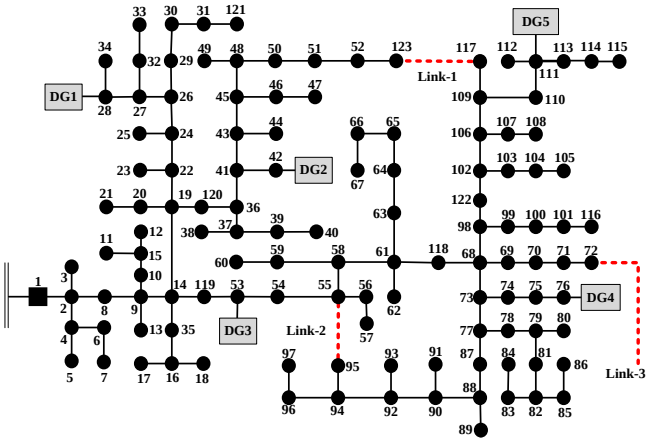

Figure 7. The modified IEEE 123-bus distribution systems in each feeder.

1) Tests in the Worst-Case Fluctuation Scenarios

Skipping 60 branches with zero restorable power and two link lines, the simulation results of "N-1" scan conducted in Feeder A are shown as Fig 8, when the restoration strategies of DROM and RROM are implemented under the worst-case scenarios.

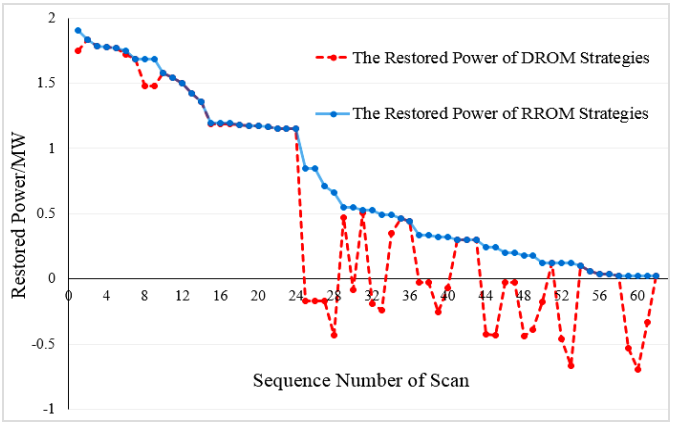

Figure 8. A restoration performance comparison between the DROM and RROM under the worst-case fluctuation scenarios in the "N-1" scan of Feeder A. The x-axis is the sequence number of the scan in decreasing order of the restored power of RROM strategies. The y-axis is the final restored power, in units of MW.

In Fig 8, the solid blue curve and the dashed red curve represent the final restored power of RROM and DROM, respectively. It was obvious that RROM performed much more robust than DROM in the worst-case conditions, and recovered more outage power in 30 cases among the overall 62 testcases. The feasibility and optimality of RROM strategies were guaranteed at all times. While it caused that failures occurred in 23 cases using DROM strategies, inducing extra load shedding. The aggregate restoration results of DROM and RROM are summarized in Table VIII.

TABLE VIII.
RESTORATION COMPARISON OF DROM AND RROM IN THE "N-1" SCAN OF FEEDER A UNDER THE WORST-CASE FLUCTUATION SCENARIOS

Model	Number of failures	Success rate	Total restored power (MW)	Number of cases with higher restored power

DROM	23	62.9%	31.476	0
RROM	0	100%	46.397	30

2) Tests Using Monte Carlo Simulations

Another restoration "N-1" scan is carried out in Feeder A of the double-feeder distribution system using Monte Carto simulations. Each contingency case is tested for 2000 fluctuation scenarios, which are generated independently and randomly in Gaussian distributions within the 3σ intervals of expression (31). Four typical cases are chosen to summarize the simulation results, including branch 19A-22A (A means that the corresponding bus lies in Feeder A, so does B), branch 61A-62A, branch 73A-74A, and branch 94A-96A, as presented in Table IX.

TABLE IX.
MONTE CARLO SIMULATION RESULTS USING DROM AND RROM FOR RESTORATION IN FIVE TYPICAL CASES OF FEEDER A

Faulty Branch	Model	Success rate	Average restored power $\bar{P}$ (MW)	Disconnected branches in restoration strategies
ln73A-74A (Type I)	DROM	96.25%	0.634715	ln94B-95B, ln61A-118A, ln61B-118B, ln72A-72B
	RROM	100%	0.66	ln51A-52A, ln94B-95B, ln117B-123B, ln72A-72B
ln94A-96A (Type I)	DROM	90.55%	0.0166906	ln19A-120A, ln61B-118B, ln55B-95B, ln72A-72B
	RROM	100%	0.02	ln52A-123A, ln94B-95B, ln117B-123B, ln72A-72B
ln61A-62A (Type II)	DROM	100%	1.68242	ln70B-71B, ln77B-87B, ln55A-95A, ln117B-123B
	RROM	100%	1.685	ln48A-50A, ln69B-70B, ln90B-92B, ln102B-122B
ln19A-22A (Type III)	DROM	100%	0.85	ln90A-92A, ln88B-90B, ln68B-118B, ln72A-72B
	RROM	100%	0.85	ln68A-69A, ln68A-73A, ln68B-73B, ln98B-122B

These testcases are classified into three types according to their results. As for Type III, the restoration performances of DROM and RROM strategies are observed to be the same. While RROM achieved a 100% success rate in all cases, and gained more average restored power than DROM in Type I and II. Once again, above simulation results verified the robustness and optimality of RROM.

G. Computational Efficiency

Numerical simulations are implemented in a computing environment with Intel(R) Core(TM) i7-4510U CPUs running at 2.60 GHz and with 8-GB RAM. We use Microsoft Visual Studio 2010 for programming and solved using IBM ILOG CPLEX 12.5. Regarding the modified PG&E 69-bus system, it takes 2.3 seconds on average to complete a DROM process, including model building and solution, while the average CPU time is 20.8 seconds for RROM, which generally converges in one or two iterations. In terms of the 246-bus test system, the average CPU time is 3.5s and 130.3s for DROM and RROM, respectively. Actually, the computing time heavily relies on the scale of potential solution space. Although the branch-and-bound algorithm will consume significantly more time with increasing size of problems, distribution networks can operate in a decentralized manner [28] [29] and the real scale in restoration make RROM acceptable. Some speedup algorithms introduced in [15] can be utilized to improve the computational efficiency.

V. CONCLUSION

Uncertainty factors of DG outputs and load demands in active distribution network restoration bring challenges to traditional deterministic methods. To incorporate these uncertainties, we propose a two-stage adaptive robust restoration optimization model, formulated as a mixed integer linear programming problem, whose solution can be obtained using the column-and-constraint method. The implementation of this robust method is tested on a modified PG&E 69-bus system and a 246-bus distribution system. The results of numerical tests indicate that the restoration strategies generated from our model are robust under fluctuating DG outputs and time-varying load demands, and are feasible for all scenarios in the predefined uncertainty sets. The superiority of our model is validated in comparison with a deterministic model for restoration performance.

REFERENCES

[1] D.S. Popovic, R.M. Ciric, "A multi-objective algorithm for distribution networks restoration," *IEEE Trans. Power Del.*, vol. 14, no. 3, pp. 1134-1141, Jul 1999.

[2] A.L. Morelato, A. Monticelli, "Heuristic search approach to distribution system restoration," *IEEE Trans. Power Del.*, vol. 4, no. 4, pp. 2235-2241, Oct 1989.

[3] N.D.R. Sarma, V.C. Prasad, K.S. Prakasa Rao, V. Sankar, "A new network reconfiguration technique for service restoration in distribution networks," *IEEE Trans. Power Del.*, vol. 9, no. 4, pp. 1936-1942, Oct 1994.

[4] D. Shirmohammadi, "Service restoration in distribution networks via network reconfiguration," *IEEE Trans. Power Del.*, vol. 7, no. 2, pp. 952-958, Apr 1992.

[5] T.D. Sudhakar, N.S. Vadivoo, S.M.R. Slochanal, "Heuristic based strategy for the restoration problem in electric power distribution systems," in, *2004 International Conference on Power System Technology*, vol. 1, pp. 635-639, 21-24 Nov. 2004.

[6] S. Toune, H. Fudo, T. Genji, Y. Fukuyama, Y. Nakanishi, "Comparative study of modern heuristic algorithms to service restoration in distribution systems," *IEEE Trans. Power Del.*, vol. 17, no. 1, pp. 173-181, Jan 2002.

[7] W.P. Luan, M.R. Irving, J.S. Daniel, "Genetic algorithm for supply restoration and optimal load shedding in power system distribution networks,", *IEE Proceedings- Generation, Transmission and Distribution*, vol. 149, no. 2, pp. 145-151, Mar 2002

[8] Y. Kumar, B. Das, J. Sharma, "Multiobjective, Multiconstraint Service Restoration of Electric Power Distribution System With Priority Customers," *IEEE Trans. Power Del.*, vol. 23, no. 1, pp. 261-270, Jan. 2008

[9] Y.-Y. Hsu, H.-M. Huang, "Distribution system service restoration using the artificial neural network approach and pattern recognition method," *IEE Proceedings- Generation, Transmission and Distribution*, vol. 142, no. 3, pp. 251-256, May 1995

[10] Y. Huang, S. Chen, C. Huang, "Evolving radial basic function neural network for fast restoration of distribution systems," in *2011 6th IEEE Conference on Industrial Electronics and Applications (ICIEA)*, pp. 401-406, 21-23 June 2011

[11] C. C. Liu, S. J. Lee, S.S. Venkata, "An expert system operational aid for restoration and loss reduction of distribution systems," *IEEE Trans. Power Syst.*, vol. 3, no. 2, pp. 619- 626, May 1988.

[12] C.S. Chen, C.H. Lin, T.T. Ku, M.S. Kang, C.Y. Ho, C.F. Chen, "Rule-based expert system for service restoration in distribution automation systems, "in *2012 IEEE International Conference on Power System Technology (POWERCON)*, pp. 1-6, Oct. 30 2012-Nov. 2 2012.
[13] J.A. Taylor, F.S. Hover, "Convex Models of Distribution System Reconfiguration," *IEEE Trans. Power Syst.*, vol. 27, no. 3, pp. 1407-1413, Aug. 2012.
[14] R.A. Jabr, R. Singh, B.C. Pal, "Minimum Loss Network Reconfiguration Using Mixed-Integer Convex Programming," *IEEE Trans. Power Syst.*, vol. 27, no. 2, pp. 1106-1115, May 2012.
[15] K. Chen, W. Wu, B. Zhang, H. Sun, "Security evaluation for distribution power system using improved MIQCP based restoration strategy," In *2014 IEEE PES Innovative Smart Grid Technologies Conference (ISGT)*, pp. 1-6, 19-22 Feb. 2014.
[16] C. D'Adamo, S. Jupe, C. Abbey, "Global survey on planning and operation of active distribution networks - Update of CIGRE C6.11 working group activities," Electricity Distribution - Part 1, 2009. CIRED 2009. 20th International Conference and Exhibition on, vol., no., pp. 1-4, 8-11 June 2009.
[17] D. S. Popovic, Z. N. Popovic, "A risk management procedure for supply restoration in distribution networks," *IEEE Trans. Power Syst.*, vol. 19, no. 1, pp. 221-228, Feb. 2004
[18] W.-H. Chen, M.-S. Tsai, H.-L. Kuo, "Distribution system restoration using the hybrid fuzzy-grey method," *IEEE Trans. Power Syst.*, vol. 20, no. 1, pp. 199-205, Feb. 2005
[19] H.-C. Kuo, Y.-Y. Hsu, "Distribution system load estimation and service restoration using a fuzzy set approach," *IEEE Trans. Power Del.* vol. 8, no. 4, pp. 1950-1957, Oct 1993
[20] K. Chen, W. Wu, B. Zhang, H. Sun, "Robust Restoration Decision-Making Model for Distribution Networks Based on Information Gap Decision Theory," *IEEE Trans. on Smart Grid*, vol. 6, no. 2, pp. 587-597, Feb., 2015.
[21] C. Lee, C. Liu, S. Mehrotra, Z. Bie, "Robust Distribution Network Reconfiguration," *IEEE Trans. on Smart Grid*, vol. 6, no. 2, pp. 836-842, Mar., 2015
[22] D. Bertsimas, M. Sim, "The price of robustness," *Operations research*, vol.52, no. 1,pp.35-53, 2004.
[23] M. Lavorato, J.F. Franco, M.J. Rider, R. Romero, "Imposing Radiality Constraints in Distribution System Optimization Problems," *IEEE Trans. Power Syst.* , vol.27, no.1, pp.172-180, Feb. 2012.
[24] B. Zeng, L. Zhao, "Solving two-stage robust optimization problems using a column-and-constraint generation method," *Operations Research Letters*, vol. 41, no.5, pp. 457-461, 2013.
[25] V. Gabrel, M. Lacroix, C. Murat, N. Remli, "Robust location transportation problems under uncertain demands," *Discrete Applied Mathematics*, vol. 164, no.1, pp. 100-111, 19 February 2014.
[26] M.E. Baran, F.F. Wu, "Optimal capacitor placement on radial distribution systems," *IEEE Trans. Power Del.*, vol. 4, no. 1, pp. 725-734, Jan 1989.
[27] (Oct. 14, 2015). [Online]. Available: https://drive.google.com/file/d/0BzBNHekT7PzcYk1yUzFBN1BldTQ/view?usp=sharing
[28] F. Ding, K.A. Loparo, "Decentralized network reconfiguration and restoration for smart distribution systems — Part I: Decentralized approach," In 2014 IEEE PES T&D Conference and Exposition, pp. 1-5, 14-17 April 2014
[29] F. Ding, K.A. Loparo, "Hierarchical Decentralized Network Reconfiguration for Smart Distribution Systems—Part I: Problem Formulation and Algorithm Development," *IEEE Trans. Power Syst.*, vol. 30, no. 2, pp. 734-743, Mar., 2015

BIOGRAPHIES

Xin Chen received the B.S. degree in engineering physics from Tsinghua University, Beijing, China, in 2015, where he is pursuing the Master degree. His research interests include active distribution networks planning and operation optimization.

Wenchuan Wu (SM'14) received the B.S., M.S., and Ph.D. degrees from the Electrical Engineering Department, Tsinghua University, Beijing, China.

Currently, he is a Professor with the Department of Electrical Engineering, Tsinghua University. His research interests include energy management system, active distribution system operation and control, and EMTP-TSA hybrid real-time simulation. He is an associate editor of *IET Generation, Transmission & Distribution* and editor of *Electric Power Components and Systems*.

Boming Zhang (SM'95–F'10) received the Ph.D. degree in electrical engineering from Tsinghua University, Beijing, China, in 1985. Since 1985, he has been with the Electrical Engineering Department, Tsinghua University, promoted to a Professor in 1993. His interest is in power system analysis and control, especially in the EMS advanced applications in the Electric Power Control Center (EPCC).